

# A Case Study of a Methodological Approach to the Verification of UAV Propeller Performance

Goran Vorotović\* – Jela Burazer – Aleksandar Bengin – Časlav Mitrović –  
Miloš Januzović – Nebojša Petrović – Đorđe Novković  
University of Belgrade, Faculty of Mechanical Engineering, Serbia

*Understanding the behaviour of propeller-driven aircraft has been the primary goal of aviation since the brothers Orville and Wilbur Wright. Traction characteristics, which have over time become dominant in the field of aviation in addition to thrust, both examined and analysed, nevertheless represent a sort of oxymoron in modern aviation. In this sense, the authors of the paper present the possibilities of static performance characteristics and vibrations of aircraft propellers through the analysis of low-powered aircraft. The use of low-powered aircraft as “expendable” material is the reality we live in, but ensuring the safety of their use is the primary goal of the researchers who deal with this issue. Accordingly, the authors of this paper present indications of the methodology of testing the blades of low-power aircraft in the atmosphere with an observation that the same indications can be used with aircraft of higher power, as well as with the aircraft on celestial bodies that have not been tested or available. A test bench for the quantification of thrust force, torque, and vibration of small unmanned aerial vehicles’ (UAV) vehicle propellers is presented. The obtained results realistically describe the complex behaviour of propellers in operation.*

**Keywords:** propeller, traction-dynamic characteristics, oscillations, acquisition, dynamics

## Highlights

- A test bench for testing the propellers of low-power UAV vehicles was designed.
- A complete methodology for testing low-power UAV propellers using simple measuring techniques was developed.
- The acquired experimental data realistically describe the complex behaviour of propellers in operation.

## 0 INTRODUCTION

Small unmanned aerial vehicles (UAV) propeller design should reflect the optimal choice of aerodynamics, structural analysis, dynamic analysis, material selection, production technology, cost and dynamic traction characteristics. The aerodynamic design of the propeller is based on the choice of airfoil, chord, and pitch-angle radial distributions.

Particular attention is paid to the reliability, the noise level, the aesthetic appearance of the blade, the functional dependence of traction forces, the torques, the number of revolutions and the power of the power unit for all test conditions. One of the important requirements when designing a propeller is the maximum reliability of the structure in all modes of exploitation. Such optimization requires the inclusion of all parameters through aerodynamic and structural modelling and the adoption of all major components of the system that include the use of propellers.

An error that would appear in the production of the propeller would have the effect of endangering the safety and reliability of the operation of the unmanned aerial vehicle due to an increase in stress and deformations, a loss of traction force, and even breakage of the propeller. Less extreme consequences include reduced efficiency and performance of

the drone, shortened service life, and increased maintenance costs.

There are several theories that can be used for the determination of the aerodynamic characteristics of small UAVs: blade element theory (BET) [1] and [2], vortex methods [3] and computational fluid dynamics (CFD) [4] to [7]. Each of them has some disadvantages. Specifically, the BET and vortex methods have low or medium accuracy on the near-flow solution. Additionally, maximum values of lift and viscous drag coefficients cannot be calculated [8] and [9]. These values are important parameters for UAV design, flight control and performance studies. CFD is gaining popularity in the development of modern UAVs [10]. The numerical verification of UAV propeller performance using computational fluid dynamics (CFD), although of high accuracy, is dependent on the selected turbulence model and the selected mesh and is computationally expensive. Furthermore, numerical models require experimental validation. Experimental verification of UAV propeller performance can be done using wind tunnels [11] and dynamic testing, including model analysis and structural testing [12]. In addition to laboratory testing, verification of UAV propeller performance can be done using flight testing and data analysis [13].

Because unmanned aerial vehicles are currently viewed as devices for “one-time” use only, the

testing of the components of such aircraft, including propellers, has been relegated to the background to the detriment of the safety of air traffic and elements on the ground. As propellers are the only propulsion source for UAVs, any problem that would appear on the propeller would affect the UAV as a whole [14]. In this context, safety is set as a primary task; accordingly, an increasing number of manufacturers and institutions dealing with this issue have decided to build test benches for testing the static performance characteristics and vibrations of propellers of small unmanned aircraft. Some of these results are presented in [15] and [16].

The subject of this paper is the presentation of a methodology for low-power UAV propeller testing, taking into account their dynamic traction characteristics. More precisely, the research aims to determine the value of thrust force and vibration level, as well as the functional dependence of forces, revolutions per minute  $RPM$  [ $\text{min}^{-1}$ ], power, and torque by applying simple measuring techniques.

## 1 TEST BENCH DESCRIPTION

The test bench for testing the static performance characteristics and vibrations of small UAV propellers is made of aluminium construction (Fig. 1) that can safely test propellers with a diameter of up to 550 mm. The supporting construction of the test bench in question is made of aluminium L profiles with dimensions of  $30 \text{ mm} \times 50 \text{ mm} \times 5 \text{ mm}$ . Preliminary calculations of the structure's static and dynamic load-bearing capacities have shown satisfactory results that are in accordance with positive engineering practice related to statics and dynamics as a whole, with a degree of safety of 1.6.

The power group consists of one 250 W alternating current motor (2), controlled by a precise alternating current regulator (8) in the range from 0 V to 300 V. The regulator is a torus type and ensures a continuous change of the operating voltage. The motor is installed in an aerodynamic formwork made of aluminium, which is placed on an aerodynamic

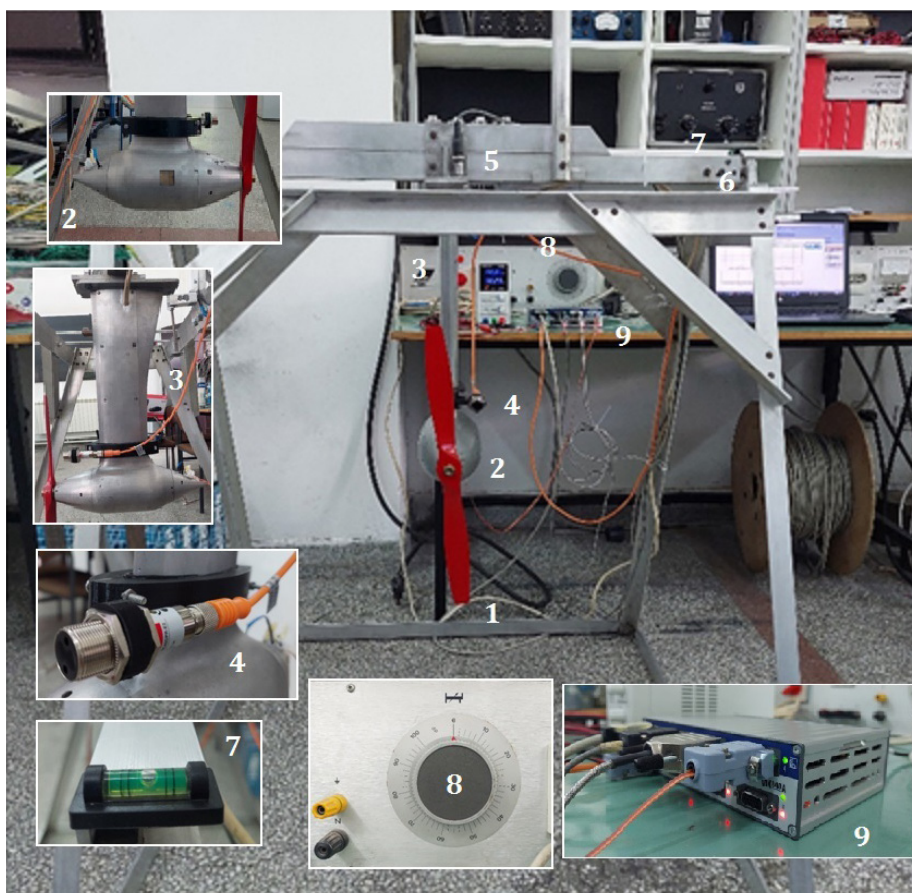


**Fig. 1.** Experimental rig: 1 propeller, 2 motor, 3 pylon, 4 optical encoder, 5 and 6 accelerometers, 7 scale, 8 alternating current regulator, and 9 central acquisition unit

support, a pylon (3). For fine adjustment of the zero-balance position of the propeller, a precision scale (7) is used, which is an integral part of the test bench.

The propeller is placed on the test bench by means of a conical holder on the drive shaft, which is secured with a self-locking nut. It is important to note that any propeller imbalance will be detected by the vibration detection system that is an integral part of the test bench and will be described later.



Fig. 2. Load cell for thrust force measurement

The HBM QuantumX MX-840A central acquisition unit (9) is a multifunctional model of receiving analogue and digital signals with the parallel tracing of the input quantities flow, an integrated microcomputer, offloading the acquisition bus with a higher-level system and enabling the transient flow of signals from specific “smart sensors” directly to the control unit.

The acquisition unit is equipped with a LAN and FireWire bus for distributing information to a higher-order system (acquisition computer) as well as for expanding the number of measurement points by direct connection to several Quantum devices. HBM QuantumX MX840A is a multi-channel acquisition unit intended for static and dynamic parallel measurements. Due to the integration with a personal computer as a higher-order system, the measurement process is extremely simple, and the complete acquisition system is compact and small in size. This eight-channel acquisition unit provides 20,000 measurements per second per channel with 24-bit resolution. All 8 A/D converters work synchronously and monitor the transformation of physical quantities into a digital signal in real time.

To measure the thrust force, a console-type force transducer, shown in Fig. 2, was used. It was placed at a distance of  $a = 105$  mm from the central axis of the pylon (see Fig. 3). The force transmitter is made of aluminium, and two  $120 \Omega$  strain gauges are placed on it in the axial direction of the transmitter. Two  $120$

$\Omega$  resistors are placed on the transducer to form a full Wheatstone bridge. The transmitter is connected to the acquisition unit according to the manufacturer’s factory specification [17]. The measuring bridge is supplied with a DC input voltage  $V_I$ , while the output voltage  $V_O$  depends on the changes in the resistance of the strain gauges due to their deformations and is proportional to the value of the bending force acting on the transducer. By changing the voltage using the voltage regulator, the value of the number of revolutions of the propeller changes and thus the traction force. The maximum load value on the force sensor is 100 N.

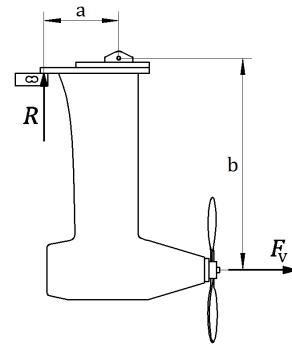


Fig. 3. Forces on the test bench

Fig. 3 shows that the thrust force is the result of the rotation of the propeller, which is mounted on two different arm lengths, with the arm of the pylon  $b$  being longer than the arm of the measuring device component. With this in mind, the real thrust force is calculated by applying the expression:

$$F_v = \frac{a}{b} R = \frac{105}{442} R = 0.237R. \quad (1)$$

A LANELO PR18-BC40DPR-E2 optical digital encoder (position (4) in Fig. 1) with a maximum response speed of 400 Hz was used to measure the number of revolutions, which provided a range of revolutions measuring up to  $12000 \text{ min}^{-1}$ . The digital encoder is placed on an aerodynamic support that follows the contour of the pylon and has the ability to change the distance of the sensor in relation to the propeller for precise adjustments of the measured response.

Two accelerometers are used for vibration measurements: MONITRAN MTN/7100-50 (position (6) in Fig. 1) with a measurement range of  $-50$  g to  $+50$  g and a response speed of 1000 Hz, and HBM 1-B12/200 (position (5) in Fig. 1) with a measurement range of  $-20$  g to  $+20$  g with a response speed of 100 Hz. These accelerometers are placed on two

predefined points on the structure itself (Fig. 4). One is placed on the part of the bench that is affected by the thrust force of the propeller (i.e., the non-fixed part of the construction), while the other is placed on the fixed part of the test bench.

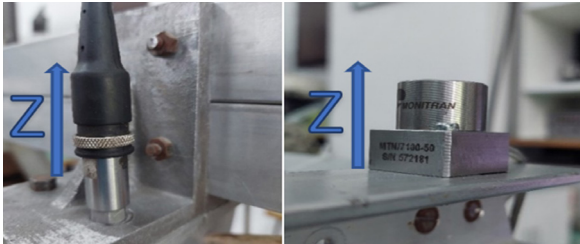


**Fig. 4.** Accelerometers (HBM and Monitran) with orientation of the z-axis

A special console support for torque measurement is designed and manufactured. Two 120  $\Omega$  strain gauges are mounted on this support and are connected to the acquisition device with a Wheatstone half-bridge (Fig. 5).

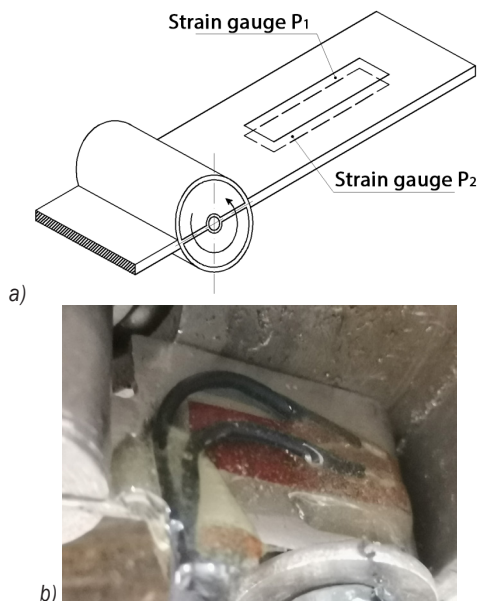


**Fig. 5.** Strain gauge on the console support; a) schematic and b) real

All previously mentioned sensors are calibrated before putting the test bench into operation, and their characteristics are entered into the CATMAN EASY acquisition software database. The calibration of the digital encoders is regulated by a simple display of counters per unit of time, while the calibrations of force and torque transmitters are done by entering loads with standard weights and using the HIOS HP-20 torque calibrator, respectively. Calibration of the

accelerometers is performed by placing the sensor in three positions (two sensors placed in the direction of the g component and one directed in that direction).

## 2 TESTING METHODOLOGY

A propeller that is prepared for testing is placed on the drive shaft of a motor by means of a conical holder and is secured with a self-locking nut. Since this test bench can be used for the testing of propellers of a wide range of diameters, which are of different geometries, they also differ in their mass. This is why this test bench has scales (7), by means of which we adjust the position of the non-fixed part of the structure to be in perfect balance. In that way, we are absolutely sure that the propeller is in its zero-level position and that once it starts to rotate, the produced thrust force will be immediately transferred to the load cell shown in Fig. 2. Once the test bench is set in zero balance with the testing propeller mounted on the motor driving shaft, we can proceed to data acquisition.

The sensors connected to the QuantumX acquisition unit are thrust force transducer, fixed and non-fixed accelerometer, strain gauge for torque measurement and optical encoder for *RPM* measurement. In order to avoid any error accumulation that could emerge on the sensor, the output of force and torque sensors in the sensor list are set to zero before the actual measurement session.

Fig. 6 shows the working screen of the CATMAN EASY software during propeller testing. For a defined *RPM*, changes are monitored on the transmitters of thrust force, torque, and vibrations, whose signals are incorporated into the corresponding graphic displays. The vibrations diagram that can be seen in Fig. 6 corresponds to the accelerometer that is placed on the non-fixed part of the test bench. The green button on the right monitors the signals from both accelerometers. In the case of a resonance of these two sensors, the green button becomes red, and the experiment is terminated.

In this manner, in case of any unforeseen circumstances, uncontrolled and unexpected increase/decrease of some of the observed quantities, or in the case of a resonant behaviour in the test bench, the experiment is terminated in a timely manner. All values can be exported in files of different formats (xlsx, ASCII, Matlab, etc.) for further analysis.

This test bench is located in an underground facility within a wind tunnel. This means that the test conditions have an environmental temperature of 20  $^{\circ}\text{C}$  and air humidity of 50 %. The values of these

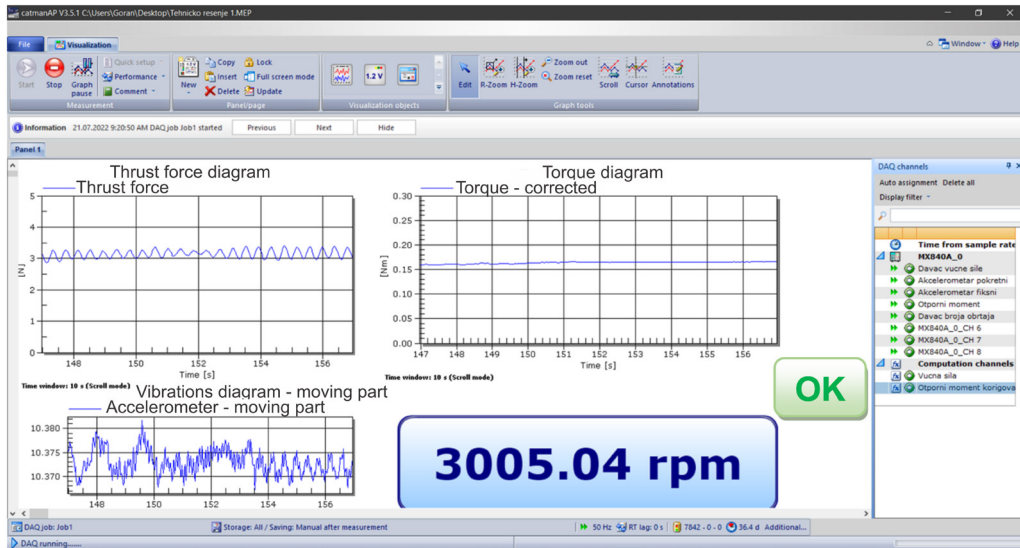


Fig. 6. CATMAN EASY working environment

two parameters are monitored constantly and are constant in time.

### 3 RESULTS AND DISCUSSION

Confirmation of the proposed methodology was carried out using measurements on the propeller shown in Fig. 7, whose characteristics are given in Table 1.

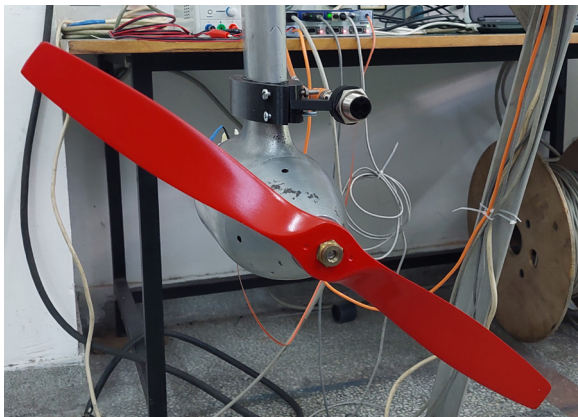


Fig. 7. Propeller on the test bench

During the trial measurements, it was determined that at a higher RPM, significantly greater vibrations occur in the system. Taking that into consideration and keeping in mind the safety of the experiment, it was decided to test the propeller in question for the four values of the RPM shown in the Table 2.

Table 1. Test propeller characteristics

Diameter, $D$	420 mm
Number of blades	2
Airfoil	Clark-Y
Reference pitch angle at $3/4D$	$19^\circ$

Table 2. RPM in the experiment

$RPM_1$ [min <sup>-1</sup> ]	$RPM_2$ [min <sup>-1</sup> ]	$RPM_3$ [min <sup>-1</sup> ]	$RPM_4$ [min <sup>-1</sup> ]
1000	2000	3000	3200

Data processing was performed with a maximum sampling rate of 20 kHz per channel. For the test in question, the sampling rate was 50 Hz. A Butterworth filter at 50 Hz with fully digital-to-analogue conversion distributed over a 400 MB/s fire-wire protocol is used.

Fig. 8 shows the diagrams of the comparative time dependence of the signal from the vibration transmitter and the optical encoder used to measure the RPM of the propeller. For all series of measurements, it is observable that increased vibrations occur at 2000 min<sup>-1</sup>, which indicates the asymmetry of the tested propeller.

The diagram of the dependence of the thrust force on the RPM is shown in Fig. 9, from which it can be concluded that the repeatability of the results is at a high level, which was verified by calculating the degree of correlation. For each of the series of measurements, the achieved degree of correlation was 0.98.

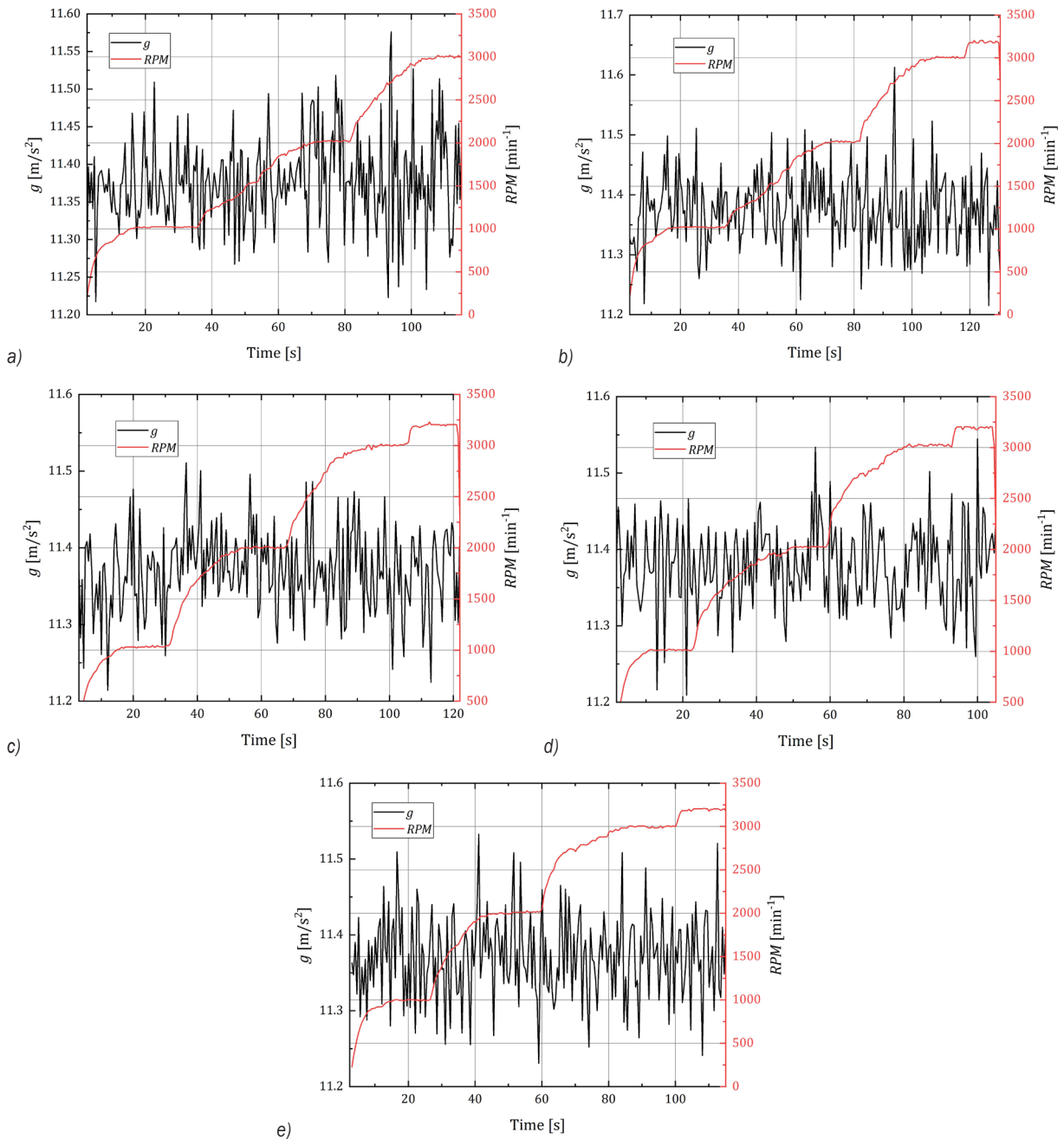


**Fig. 8.** Signal from accelerometer with the change in RPM: a) series 1, b) series 2, c) series 3, d) series 4, and e) series 5:  $g$  [m/s<sup>2</sup>] – acceleration

Two accelerometers are used in order to identify the interference between the operation of the propeller and the supporting structure. The experiment showed that there is no even linear dependence between the propeller's rpm and the response of the thrust force transducer. The pylon is of aerodynamic form and, as such, its geometry calms the airflow after the propeller.

As can be seen from Fig. 9, the thrust force is a square function of the RPM, as predicted by theory. With an increase in RPM, the thrust force is increased, since the propeller blades rotate faster, thus increasing the air mass flow rate flowing against them. The consequence of this is the increase of the forward load applied to the propeller that acts as a moving force forward. Due to the construction of the test bench and

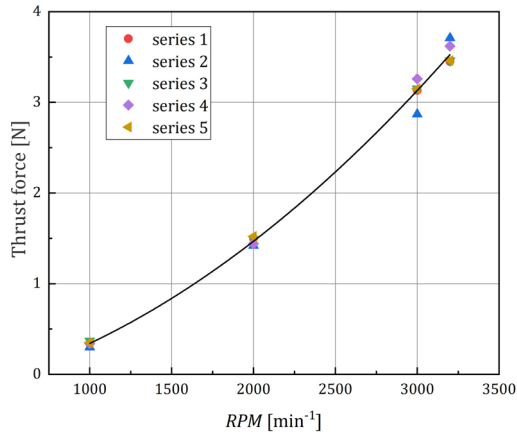


Fig. 9. Thrust force for different values of RPM

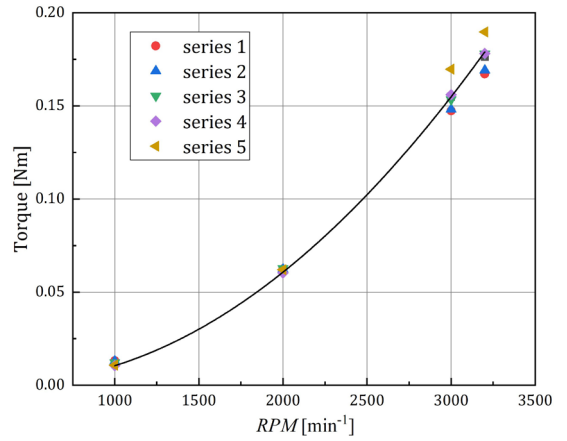


Fig. 10. Torque for different values of RPM

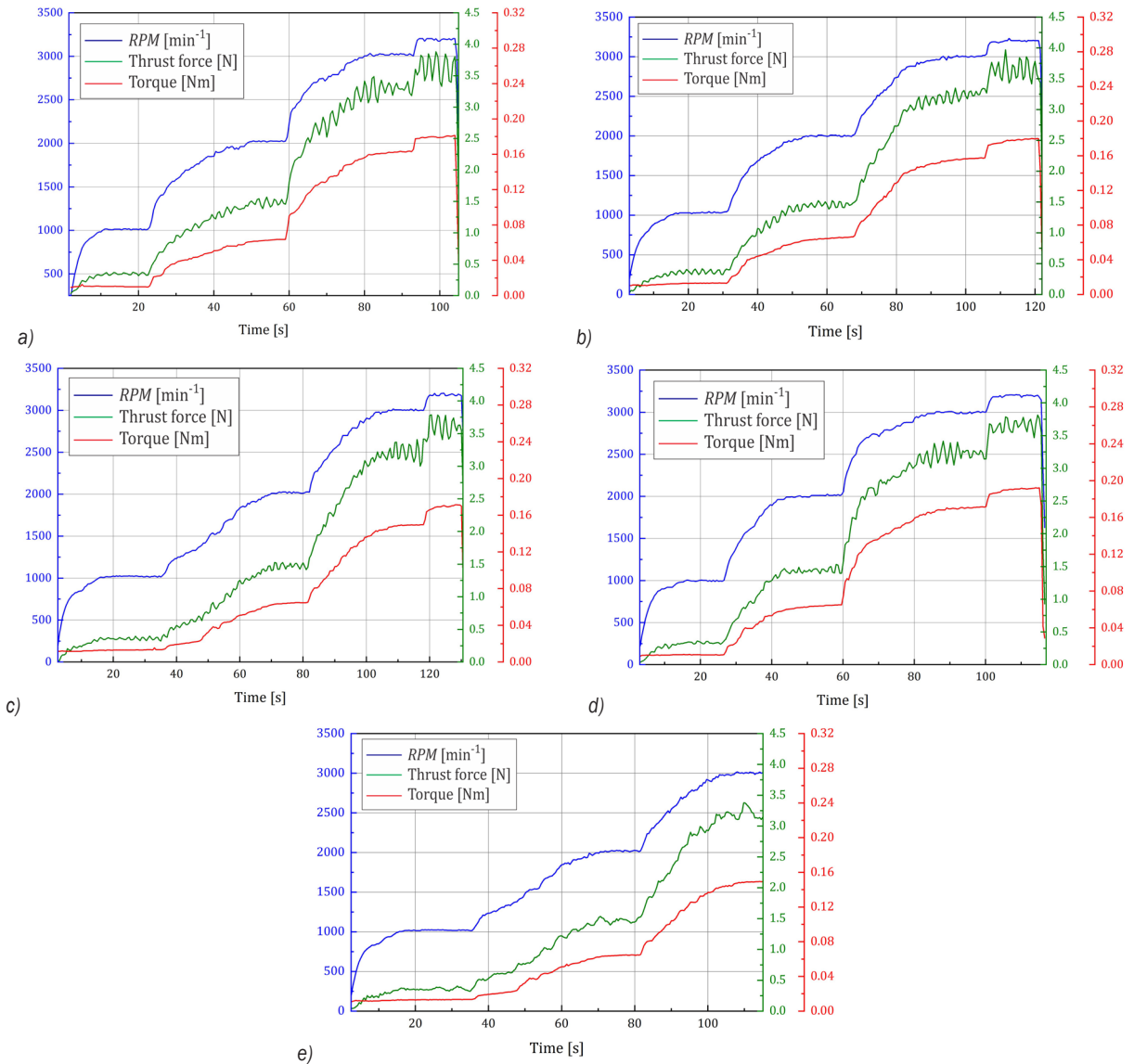


Fig. 11. Time evolution of RPM, thrust and torque: a) series 1, b) series 2, c) series 3, d) series 4, and e) series 5

the position of the load cell, this motion is restricted by the load cell itself. Hence, the load cell is “perceiving” the thrust force acting on the propeller. Fig. 10 shows the dependence of the resistance torque on the *RPM*. A slightly higher dispersion of the measured values is observed here, with a degree of correlation of 0.96.

The main discrepancy in the results is for higher *RPMs*. This behaviour of the value of the torque can be attributed to the inadequate stiffness of the console support on which the strain gauges are placed, which is reflected in conditions of increased vibration of the test bench. Therefore, these results are another indicator of the quality of the propeller under the test.

Fig. 11 shows the time dependences of the signals from the traction force sensor and the resistive torque sensor for all realized *RPM* and all series of measurements. A trend of global “tracking” of the values of both traction force and torque with the change in the number of revolutions is noticeable. Instability is also observed on the signal of the traction force sensor in the areas of the number of revolutions over 2000  $\text{min}^{-1}$ , which is a consequence of increased vibrations on the test table due to the imperfection of the tested propeller.

From the previously presented results, it can be concluded that the test table that is the subject of this technical solution can be used both for testing the static performance characteristics and vibrations and for balancing the propellers of unmanned aerial vehicles.

#### 4 CONCLUSIONS

This test aims to define the static performance characteristics and vibrations of propellers and to determine the functional dependence of force, *RPM*, power, torque, as well as the vibration level, especially from the point of view of use by propeller manufacturers in terms of quality checking, load capacity and traction-dynamic characteristics. In contrast, the results of vibro-diagnostic parameters are significant in terms of their balance and potential resonance. Not less significant is the educational and scientific research aspect from the point of view of aviation and information technologies development. The applied methodology represents a high-quality process of evaluating propeller parameters both in real conditions of exploitation and in laboratory conditions.

After testing, the acquired experimental data realistically describe the complex behaviour of propellers in operation. The experimental results represent the basis for finding the parameters that

cause the improper operation of propellers, as well as the quality characterization procedures for determining the service life of propellers from the aspect of dynamic traction characteristics in the initial phase of development.

The results of the research indicate the need to verify the obtained results in real operating conditions, where the combination of hardware and software components would provide the possibility of verifying analytical and experimental results from the test bench with real parameters in real operating conditions. In this sense, the authors are of the opinion that a real confirmation of the results on real aircraft in all atmospheric conditions is needed, regardless of the planet on which the experiment is performed.

#### 5 ACKNOWLEDGEMENTS

This research was funded by a grant from the Ministry of Education, Science and Technological Development, Republic of Serbia, under Contract No. 2022451-03-68/2022-14/200105 (subprojects TR35046, TR35045, and TR35040).

#### 6 REFERENCES

- [1] Evdokimov, I. (2015.) Blade element theory in the UAV multirotor blade optimization, *International CAE Conference*, p. 19-20.
- [2] Kuitche, M.A.J., Botez, R.M., Viso, R., Maunand, J.C., Moyao, O.C. (2020). Blade element momentum new methodology and wind tunnel test performance evaluation for the UAS-S45 Balaam propeller. *CEAS Aeronautical Journal*, vol. 11, no. 4, p. 937-953, DOI:10.1007/s13272-020-00462-x.
- [3] Moffitt, B., Bradley, T., Parekh, D., Mavris, D. (2008). Validation of vortex propeller theory for UAV design with uncertainty analysis. *46<sup>th</sup> AIAA Aerospace Sciences Meeting and Exhibit*, DOI:10.2514/6.2008-406.
- [4] Vargas Loureiro, E., Oliveira, N.L., Hallak, P.H., de Souza Bastos, F., Rocha, L.M., Grande Pancini Delmonte, R., de Castro Lemonge, A.C. (2021). Evaluation of low fidelity and CFD methods for the aerodynamic performance of a small propeller. *Aerospace Science and Technology*, vol. 108, art. ID 106402, DOI:10.1016/j.ast.2020.106402.
- [5] Figat, M., Piątkowska, P. (2021). Numerical investigation of mutual interaction between a pusher propeller and a fuselage. *Proceedings of the Institution of Mechanical Engineers, Part G: Journal of Aerospace Engineering*, vol. 235, no. 1, p. 40-53, DOI:10.1177/0954410020932796.
- [6] Erkan, O., Özkan, M., Karakoç, T.H., Garrett, S.J., Thomas, P.J. (2020). Investigation of aerodynamic performance characteristics of a wind-turbine-blade profile using the finite-volume method. *Renewable Energy*, vol. 161, p. 1359-1367, DOI:10.1016/j.renene.2020.07.138.
- [7] Viola, I.M., Chapin, V.G., Speranza, N., Biancolini, M.E. (2018). Optimal airfoil shapes by high-fidelity CFD. *Aircraft Engineering*

- and *Aerospace Technology*, vol. 90, no. 6, p. 1000-1011, DOI:10.1108/AEAT-09-2017-0210.
- [8] Karali, H., Inalhan, G., Demirezen, M.U., Yukselen, M.A. (2021). A new nonlinear lifting line method for aerodynamic analysis and deep learning modeling of small unmanned aerial vehicles. *International Journal of Micro Air Vehicles*, vol. 13, p. 1-24, DOI:10.1177/17568293211016817.
- [9] Ostler, J.N., Bowman, W.J., Snyder, D.O., McLain, T.W. (2009). Performance flight testing of small, electric powered unmanned aerial vehicles. *International Journal of Micro Air Vehicles*, vol. 1, p. 155-171, DOI:10.1260/175682909789996177.
- [10] Paz, C., Suárez, E., Gil, C., Vence, J. (2021). Assessment of the methodology for the CFD simulation of the flight of a quadcopter UAV. *Journal of Wind Engineering and Industrial Aerodynamics*, vol. 218, art. ID 104776, DOI:10.1016/j.jweia.2021.104776.
- [11] Zhao, A., Zhang, J., Li, K., Wen, D. (2021). Design and implementation of an innovative airborne electric propulsion measure system of fixed-wing UAV. *Aerospace Science and Technology*, vol. 109, art. ID 106357, DOI:10.1016/j.ast.2020.106357.
- [12] Cruzatty, C., Sarmiento, E., Valencia, E., Cando, E. (2022) Design methodology of a UAV propeller implemented in monitoring activities. *Materials Today: Proceedings*, vol. 49, p. 115-121, DOI:10.1016/j.matpr.2021.07.481.
- [13] Chipade, V.S., Abhishek, Kothari, M., Chaudhari, R.R. (2018) Systematic design methodology for development and flight testing of a variable pitch quadrotor biplane VTOL UAV for payload delivery. *Mechatronics*, vol. 55, p. 94-114, DOI:10.1016/j.mechatronics.2018.08.008.
- [14] Anemaat, W.A.J., Schuurman, M., Liu, W., Karwas, A. (2017). Aerodynamic design, analysis and testing of propellers for small unmanned aerial vehicles. *AIAA SciTech Forum, 55<sup>th</sup> AIAA Aerospace Sciences Meeting*, DOI:10.2514/6.2017-0721.
- [15] Asson, K.M., Dunn, P.F. (1992). Compact dynamometer system that can accurately determine propeller performance. *Journal of Aircraft*, vol. 29, no. 1, p. 8-9, DOI:10.2514/3.46118.
- [16] Marchent, M.P. (2004). *Propeller Performance Measurement for Low Reynolds Number Unmanned Aerial Vehicle Applications*. MSc. Thesis, Wichita State University, Wichita
- [17] QuantumX, (2015). Operating Manual, HBM, from: <https://www.hbm.com/fileadmin/mediapool/hbmdoc/technical/A03031.pdf>, accessed on 2022-11-01.